Short Communication:

In Silico Study of Alkaloid Compounds from *Sida rhombifolia* (Sidaguri) as Antimalarial Agents Targeting *Plasmodium falciparum* Dihydrofolate Reductase

Arfansyah Arfansyah[1], Anisa Sepyana[1], Bahrun Bahrun[2], Muh Ade Artasasta[3], and Herlina Rasyid[1*]

[1]*Department of Chemistry, Faculty of Mathematics and Natural Sciences, Hasanuddin University, Jl. Perintis Kemerdekaan km 10, Makassar 90245, Indonesia*

[2]*Research Center for Chemistry, National Research and Innovation Agency (BRIN), KST BJ Habibie, Banten 15314, Indonesia*

[3]*Biotechnology Program, Department of Applied Science, Faculty of Mathematics and Natural Sciences, Universitas Negeri Malang, Jl. Semarang No. 5, Malang 65145, Indonesia*

* ***Corresponding author:***

email: herlinarasyid@unhas.ac.id

Received: April 29, 2025
Accepted: June 17, 2025

DOI: 10.22146/ijc.106340

Abstract: *Malaria, caused by the* Plasmodium *parasite, represents a significant global health challenge, with approximately 229 million cases reported in 2020. Current treatments include artemisinin-based combination therapy; however, drug resistance poses serious issues. Natural products, including alkaloids from* Sida rhombifolia, *particularly cryptolepine, effectively inhibit* Plasmodium falciparum *through DNA intercalation. Research indicates that mutations in the* Pf*DHFR enzyme of* P. falciparum *contribute to drug resistance, highlighting the urgent need for new inhibitors. A literature review combined with SwissADME, toxicology predictions, and molecular docking methods identified 11-cryptolepine carboxylic acid (**B1**) and* N*-trans-feruloyl tyramine (**B11**) as potential new inhibitors. The compounds exhibited binding energies of −7.22 and −8.41 kcal/mol, which are close to the native ligand (−7.31 kcal/mol). Additionally, they demonstrate favorable drug-likeness properties, indicating their potential as viable candidates for drug development. The molecular dynamics simulation for 100 ns was conducted to observe molecular interactions in a specific system dynamically. It was found that ligand **B1** has better stability compared to ligand **B11**. This compound demonstrates significant potential for advancing malaria treatment strategies. Further research and clinical evaluation are warranted to fully realize their potential and translate these findings into effective clinical interventions for combating malaria globally.*

Keywords: Sida rhombifolia*; antimalaria; Pf*DHFR enzyme; molecular docking; molecular dynamics*

■ INTRODUCTION

One of the biggest health problems in the globe is malaria. *Plasmodium* protozoa, which reproduce asexually within the human body and are spread by mosquitoes during blood feeding, are the cause of this disease [1]. Malaria continued to pose a serious threat to global health in 2023, with a projected 263 million cases and 597,000 fatalities recorded in 83 countries, representing 95% of malaria deaths (569,000) and 94% of cases worldwide (246 million) [2]. In Indonesia, malaria cases continue to rise, particularly in Eastern Indonesia. In 2022, malaria cases in Indonesia reached 443,530, with the highest number recorded in Papua at 356,889 cases [3]. Various treatments have been implemented to combat malaria, including artemisinin-based combination therapy, chloroquine, mefloquine, quinine, primaquine, and pyrimethamine [4].

Nevertheless, the *Plasmodium* protozoa have become resistant to a lot of current treatments. In order

to combat malaria, this has led to the creation of novel medications or pharmacological combinations [5]. Natural products are considered one of the safest treatments and have been used since ancient times [6]. Earlier, the most significant medications used in malaria treatment, quinine and artemisinin, were derived from natural products. Ongoing research continues to explore additional medicinal plants and their compounds for their antimalarial activity [7-8]. Potential natural antimalarial agents include *Artemisia annua* [9], and *Cryptolepis sanguinolenta* [10], among many other plant species. Developing antimalarial drugs using plants faces many challenges, including the resistance of malaria parasites to active compounds, the complexity of isolating active compounds, and the limited availability of specific plant species. Continuous innovation is needed to discover the most effective and efficient plant-based antimalarial medication. Communities have trusted sidaguri for years as an antimalarial remedy. This plant contains steroids, alkaloids, flavonoids, coumarins, and phaeophytins that are effective in preventing malaria. Alkaloids are thought to be a significant group of compounds with a variety of biological actions, most notably antimalarial activity. With nitrogen atoms in heterocyclic rings produced from amino acids, they constitute an important family of structurally varied molecules. Numerous alkaloids have been identified as having potent antimalarial properties and have been isolated from a variety of plant sources [11].

Numerous alkaloids, such as 11-cryptolepine carboxylic acid, cryptolepine, quindoline, 11-methoxyquinoline, quindolinone, cryptolepinone, and methyl ester 11-quindoline, have been found in *Sida rhombifolia* based on prior study. Cryptolepine is one of the alkaloids that has been identified to have significant antimalarial action. Through processes like DNA intercalation and inhibition of nucleic acid synthesis, cryptolepine can stop the growth of *Plasmodium falciparum*, the parasite that causes malaria [12]. The produced cryptolepine may act as a quinone reductase inhibitor [13]. Ethanol-water extracts also yield cryptolepine isolates from *S. rhombifolia*, which show a high potential for treating malaria [14].

However, an *in silico* analysis of secondary metabolites—specifically alkaloids derived from *S. rhombifolia*—has understudied. *P. falciparum*, the parasite that causes malaria, has little in common with host proteins and is involved in a number of metabolic activities. *P. falciparum* dihydrofolate reductase (*Pf*DHFR) and *P. falciparum* dihydroorotate dehydrogenase (*Pf*DHODH) are two proteins that have been confirmed to be targets for malaria treatment. The enzyme *Pf*DHFR is crucial for the biosynthesis of folate and is in charge of generating the DNA base deoxythymidine monophosphate. Additionally, *Pf*DHFR has a role in the production of amino acids and purine nucleotides. When common antifolates like trimethoprim, cycloguanil, and pyrimethamine inhibit *Pf*DHFR, they stop thymidine production, which in turn stops DNA synthesis and kills the parasite. Unfortunately, *P. falciparum* parasites have become widely resistant to these medications due to point mutations at particular amino acid residues in the wild-type active site of *Pf*DHFR, including Ala16, Ile51, Cys59, Ser108, and Ile164 [5]. Therefore, finding new *Pf*DHFR inhibitors is urgently needed due to the widespread and growing resistance to existing DHFR-targeting drugs, which results in frequent clinical failures and ineffective alternatives [15]. In contrast, *Pf*DHODH is a promising new target with several potent inhibitors in development and less current resistance in the field, though it remains an important focus for future therapies.

■ EXPERIMENTAL SECTION

Materials

The wild-type *Pf*DHFR (wt-*Pf*DHFR) structure utilized in this study was downloaded from the Protein Data Bank with PDB ID of 3QGT (http://rcsb.org/structure/3QGT). The wt-*Pf*DHFR is co-crystallized with pyrimethamine. Protein preparation involved removing all water molecules and complex ligands from the binding pockets of the protein, adding polar hydrogens, and calculating Gasteiger charges for each receptor atom to facilitate molecular docking using AutoDockTools.

Instrumentation

This study used a Windows 11 Home Single Language operating system laptop device with specifications: AMD Ryzen 3 3250U processor with Radeon Graphics CPU 2.60 GHz, 8 GB RAM, with installed software including AutoDockTools 1.5.7 [16], Avogadro 1.2.0 [17], BIOVIA Discovery Studio 2021 [18], Chimera program 1.18 [19], and YASARA Structure program [20].

Procedure

Ligand preparation, ADME, and toxicology prediction

A literature review was conducted on the alkaloids derived from *S. rhombifolia* using various extracts. The ligands, which are alkaloids from the *S. rhombifolia* plant, are presented in Table 1. Subsequently, absorption, distribution, metabolism, and excretion (ADME) predictions were performed using the SwissADME website (http://www.swissadme.ch) [21], while toxicity assessed through ProTox 3.0 webserver (https://tox.charite.de/protox3/) [22].

Protein-ligand docking

The compounds obtained from the literature review were used as ligands, and the 3D structure was downloaded from PubChem and optimized using Avogadro 1.2.0 [17] with MMFF94 method [23]. All ligands were formatted in PDB file format and prepared for docking in Chimera software [24]. The molecular docking protocol was established at the active site of the enzyme using a grid size of 40 × 40 × 40, coordinates of central grid point of maps 30.415, –29.071, 7.441, and a spacing of 0.375 Å in AutoDock4 with the assistance of AutoDockTools. The Lamarckian algorithm was employed to generate 10 conformations, and their 2D interactions of the best docking pose were visualized using Discovery Studio Visualizer.

Molecular dynamics simulation

Because of its lower binding energy, the complex of ligands **B1** and **B11** inhibits wt-*Pf*DHFR, according to molecular docking research. The structures of the two complexes and a single protein without a ligand were compared through molecular dynamics simulation. YASARA Structure program (YASARA Biosciences GmbH, Vienna, Austria) was used to perform molecular dynamics simulation [20]. Amber14 in a periodic boundary condition is the force field utilized in this investigation [25]. The system's pH and temperature were set at 7.4 and 310 K, respectively [26]. The TIP3P solvent was chosen, and counter ions Cl^- and Na^+ were introduced to each compound [27]. Every complex ran for 100 ns. The analysis of the Rg, RMSD, RMSD ligand, RMSF, and total hydrogen bond (H-bond) is done using the trajectory data.

■ RESULTS AND DISCUSSION

Ligand Preparation

The 3D structure of wt-*Pf*DHFR and native ligand (pyrimethamine) utilized in this study was downloaded from the Protein Data Bank (Fig. 1(a)). The docking procedure initiates with the redocking of the native ligand to assess the validity of the methodology employed. The results from the redocking of the native ligand yielded a RMSD of 0.28 Å, which is significantly below the threshold of 2 Å. This result supports the validity of the docking method utilized [28]. The superimpose and 2D

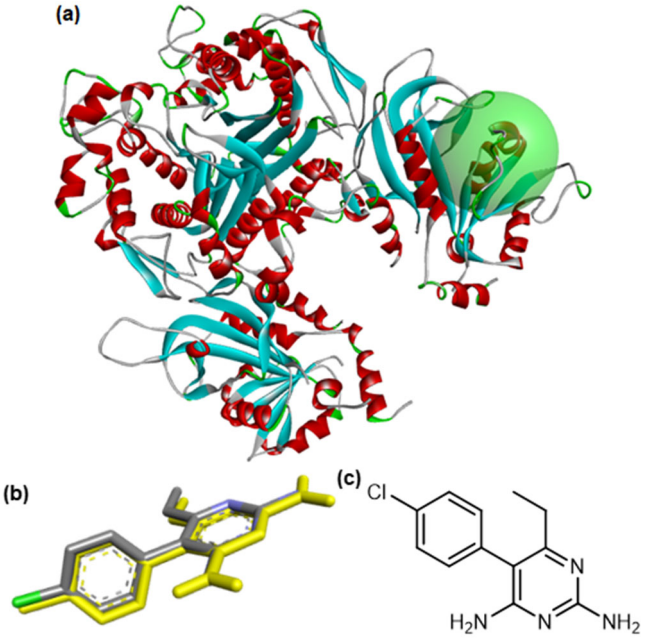

Fig 1. Structure of (**a**) protein wt-*Pf*DHFR, (**b**) superimposed structure of ligands after and before molecular docking, and (**c**) 2D structure of native ligand (pyrimethamine, CID: 4993)

Table 1. Alkaloid compounds of *S. rhombifolia*

Compound	Formula	Structure	Reference
11-Cryptolepine carboxylic acid **(B1)**	$C_{17}H_{12}N_2O_2$	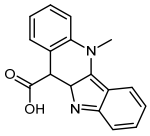	[12]
Cryptolepine **(B2)**	$C_{16}H_{12}N_2$	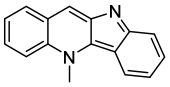	[12]
Quindoline **(B3)**	$C_{15}H_{10}N_2$	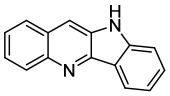	[12]
11-Methoxy-quindoline **(B4)**	$C_{17}H_{13}NO$	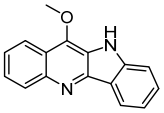	[12]
Quindolinone **(B5)**	$C_{15}H_8N_2O$	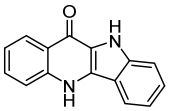	[12]
Cryptolepinone **(B6)**	$C_{16}H_{12}N_2O$	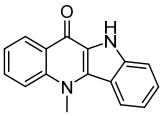	[12]
11-Quindoline methyl ester **(B7)**	$C_{17}H_{12}N_2O_2$	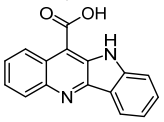	[12]
10-Methlycryptolepinone **(B8)**	$C_{17}H_{14}N_2O$	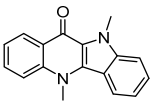	[12]
10-Ethylcryptolepinone **(B9)**	$C_{18}H_{16}N_2O$	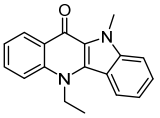	[12]
Vasicinol **(B10)**	$C_{11}H_{12}N_2O_2$	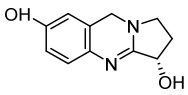	[29]
N-trans-Feruloyltyramine **(B11)**	$C_{18}H_{19}NO_4$	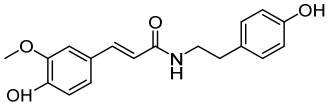	[30]
N-Methyl ephedrine **(B12)**	$C_{10}H_{15}NO$	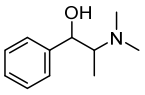	[29]
Hypaphorine **(B13)**	$C_{14}H_{18}N_2O_2$	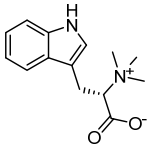	[29]
Betaine **(B14)**	$C_5H_{11}NO_2$	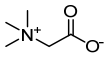	[29]
Phenethylamine **(B15)**	$C_8H_{11}N$	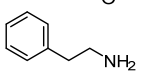	[29]
Loliode **(B16)**	$C_{11}H_{16}O_3$	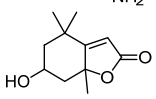	[31]

structure of the native ligand are represented in Fig. 1(b) and 1(c), respectively. The alkaloid compounds derived from *S. rhombifolia* various extract shown in Table 1.

ADME and Toxicology Prediction

In evaluating the drug-likeness of the test compounds, the determination of Lipinski's Rule of Five was conducted for oral drug candidates with biological activity in humans. This rule states that test compounds should not have a molecular weight (MW) exceeding 500 Da, as higher molecular weights reduce the concentration of the compound at the epithelial surface of the intestines, thereby decreasing absorption in the intestines and central nervous system [32]. Additionally, the rule specifies that the test compounds should not have a partition coefficient (log P) greater than 5, as a high partition coefficient indicates that the compound is lipophilic or strongly bound to membranes, making it difficult to recognize target enzymes and potentially toxic. Conversely, a too low or negative log P is also undesirable because it hinders penetration through lipid bilayer membranes [33]. Furthermore, the number of hydrogen bond donors and hydrogen bond acceptors in the compounds must be less than 5 and no more than 10, respectively. Hydrogen bond donors and acceptors represent the capacity for hydrogen bonding, where a high number of hydrogen bonds can reduce the partitioning of molecules from aqueous phases into lipid bilayer membranes for passive diffusion [34]. The lead-likeness parameter represents a molecule's ability to serve as a 'lead' in the drug discovery process [35]. The Lipinski Rules and Lead-likeness of the test compounds were summarized in Table 2.

Based on the ADME prediction for several alkaloids found in *S. rhombifolia*, it was determined that all compounds met Lipinski's rules: molecular weight ≤ 500, MlogP ≤ 4.15, N or O ≤ 10, NH or OH ≤ 5. However, only two molecules met the lead-likeness criteria: 11-cryptolepine carboxylic acid (**B1**) and *N*-trans-feruloyltyramine (**B11**). In the context of toxicology prediction, most candidate compounds are typically categorized as having inactive carcinogenicity and hepatotoxicity. Molecular docking studies further analyzed compounds that satisfy Lipinski's rules and lead-likeness parameters and demonstrate inactive toxicology. Compounds that satisfy the specified criteria specifically compounds **B1** and **B11**, exhibit favorable pharmacokinetic properties and lack significant toxic effects upon administration. This analysis is crucial as a preliminary step in screening potential drug candidates.

Table 2. Result of SwissADME and toxicology prediction

Compounds	Lipinski rules				Lead-likeness violation	Toxicology	
	MW	H-bond acceptors	H-bond donors	MlogP		Hepatotoxicity	Carcinogenicity
B1	276.29	3	1	2.81	0	Inactive	Inactive
B2	232.28	1	0	3.29	1 (MW<250)	Inactive	Inactive
B3	218.25	1	1	3.04	2 (MW<250, XlogP3>3.5)	Inactive	Inactive
B4	247.29	1	1	3.27	2 (MW<250, XlogP3>3.5)	Inactive	Inactive
B5	232.24	3	0	1.36	1 (MW<250)	Inactive	Inactive
B6	248.28	1	1	2.34	2 (MW<250, XlogP3>3.5)	Inactive	Inactive
B7	276.29	3	1	2.81	1 (XlogP3>3.5)	Active	Inactive
B8	262.31	1	0	2.58	1 (XlogP3>3.5)	Inactive	Inactive
B9	276.33	1	0	2.82	1 (XlogP3>3.5)	Inactive	Inactive
B10	204.23	3	2	0.99	1 (MW<250)	Inactive	Inactive
B11	313.35	4	3	1.89	0	Inactive	Inactive
B12	165.23	2	2	1.56	1 (MW<250)	Inactive	Inactive
B13	246.30	2	1	−2.31	1 (MW<250)	Inactive	Inactive
B14	117.15	2	0	−3.67	1 (MW<250)	Inactive	Inactive
B15	121.18	1	1	1.87	1 (MW<250)	Inactive	Inactive
B16	196.24	3	1	1.49	1 (MW<250)	Inactive	Active

Accordingly, given their favorable profiles, molecular docking analysis was performed exclusively on compounds **B1** and **B11**.

Molecular Docking Analysis

Pyrimethamine, a well-known inhibitor of wt-*Pf*DHFR and a proven anti-malarial medication, is the standard ligand used in this study. Both compounds demonstrated binding energies that were comparable to the standard ligand, according to the results of the molecular docking experiments conducted with **B1** and **B11**. **B11** obtained a considerably lower binding energy of −8.41 kcal/mol, whereas **B1** demonstrated a binding energy of −7.22 kcal/mol (Table 3). Given that the latter's binding energy surpassed that of the standard ligand, it holds substantial potential as a novel inhibitor targeting wt-*Pf*DHFR. When a ligand-receptor pair attains the lowest possible energy state, they stabilize together, resulting in decreased Gibbs free energy [36]. This observation underscores the significance of molecular docking in identifying potent inhibitory compounds capable of interacting favorably with enzymatic targets, thereby offering promising avenues for future therapeutic interventions against malaria. The detailed analysis of binding energies provides crucial insights into the stability and effectiveness of these interactions, guiding the selection of optimal candidates for further development.

The calculation of bond energy formed is a reflection of the ligand conformation within a macromolecule [37]. *N*-trans-feruloyltyramine possesses one amide functional group, two hydroxyl groups (−OH), and one methoxy group ($-OCH_3$). These three polar groups contribute to the higher affinity of **B11** compared to **B1** and the native ligand, pyrimethamine. Consequently, because of their hydrophilic nature, they affect the stability of ligand-receptor interactions [38]. Furthermore, by serving as an electron-donating group, a methoxy group added as a side chain to benzene compounds improves structural stability. Therefore, when compared to other chemicals, **B11** shows the lowest energy value. Differences in ligand binding to receptor amino acids, which establishes the most stable molecular shape, also influence the diversity in bond energy values. Furthermore, visualization analyses were conducted, as illustrated in Fig. 2, to identify the amino acids involved in inhibiting wt-*Pf*DHFR. These visualizations' outcomes show how ligands and amino acid residues interact. These amino acid connections let alpha glucosidase ligands make touch with one another, which increases their inhibitory activity [39].

Each ligand exhibits van der Waals and hydrogen bonds. As shown in Fig. 2(b), there are van der Waals interactions between **B1** and the amino acid residues of Thr185, Tyr170, Ser108, Tyr57, Asp54, Leu46, and Cys15. Furthermore, **B11** interacts with Tyr170, Ile164, Leu119, Pro113, Ile112, Ser111, Phe58, Trp48, Gly39, Cys17, and Ile14, and have an hydrogen interaction with Gly44 and Ala16 (Fig. 2(c)). The active site residues of wt-*Pf*DHFR, according to its PDBSUM entry, include Ile14, Cys15, Ala16, Asp54, Met55, Phe58, Ile164, Tyr170, and Thr185 [5]. These residues were identified through the interaction of pyrimethamine within the enzyme's active site (Fig. 2(a)). Comparing the docking results of the tested ligands with those of the standard ligand reveals that all tested ligands occupy the active site of the enzyme due to interactions with the same residues. This suggests that the binding affinities of these ligands are influenced by their ability to form stable interactions with key amino acids in the active site, thereby potentially enhancing their inhibitory efficacy against wt-*Pf*DHFR.

Molecular Dynamics Simulation

The complex of ligands **B1** and **B11** against wt-*Pf*DHFR was simulated using molecular dynamics and compared to the single protein structure. In molecular

Table 3. Molecular docking analysis

Compounds	Binding energy (kcal/mol)	Inhibition constant (nM)	H-bond interaction residue
B1	−7.22	5120	Ile14; **Asp54**; Ile164
B11	−8.41	680	Ser111; Gly166; **Asp54**; Leu40
Pyrimethamine	−7.31	4360	**Thr185**; **Ile164**; **Asp54**; **Cys15**; **Ile14**

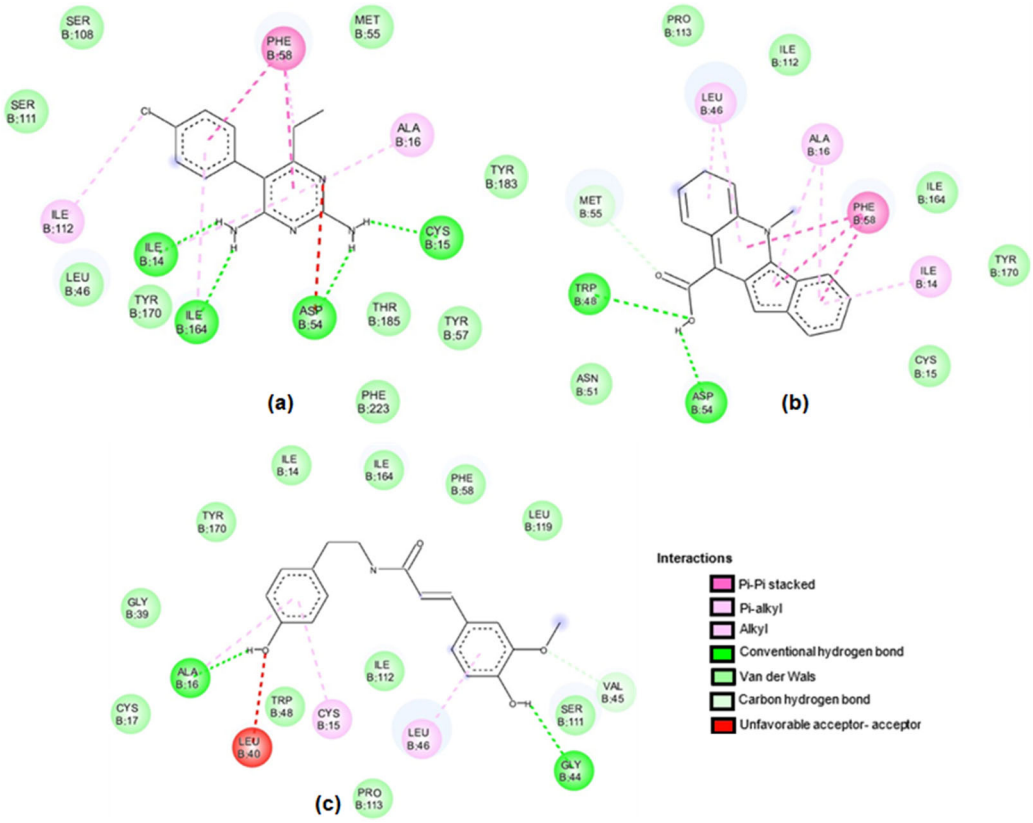

Fig 2. Two-dimensional interaction of (a) native ligand, (b) **B1**, (c) and **B11** against wt-*Pf*DHFR

docking study, these two ligands were selected because they had stronger binding affinities than the other ligands that were evaluated. One characteristic that characterizes the equilibrium conformation of an entire system is the Rg. The protein structure's folded state was indicated by the lower value, while the unfolded state was defined by the greatest value [40]. Fig 3(a) demonstrated that the Rg pattern may be enhanced by adding a ligand to the protein structure, particularly at the end of the simulation period. Based on the wt-*Pf*DHFR folding condition, complex-ligand **B1** addition to the protein structure results in a slightly better state than complex-ligand **B11**. However, the difference is not very pronounced, as clearly indicated by the observed fluctuation.

The dynamics of amino acid residues within the wt-*Pf*DHFR protein demonstrate a similar fluctuation pattern upon formation of complexes with compounds **B1**, **B11**, and native ligand (Fig. 3(b)). This observation suggests that the interactions between compounds **B1** and **B11** with the wt-*Pf*DHFR protein yield analogous effects to those produced by their respective native ligands. In contrast, analysis of the RMSD (Fig. 3(c)) reveals that compound **B11** exhibits significantly greater RMSD fluctuations, indicative of structural instability during its binding interaction with the wt-*Pf*DHFR protein. Notably, the RMSD profiles for compound **B1** and the native ligand structures display minimal fluctuations, underscoring the pronounced stability of compound **B1** throughout the simulation period.

By measuring the conformational changes of a given complex over time, the protein RMSD C-alpha determines if the simulation is in equilibrium and whether its final fluctuations are centered around a thermal average shape [41]. The RMSD C-alpha analysis results show that the fluctuation pattern of wt-*Pf*DHFR-**B1** is similar to the fluctuation pattern of the wt-*Pf*DHFR protein. The addition of ligands to both protein complex structures did not show significant changes in RMSD values. However, the fluctuation pattern in RMSD during the simulation process shows that wt-*Pf*DHFR-**B1** reached

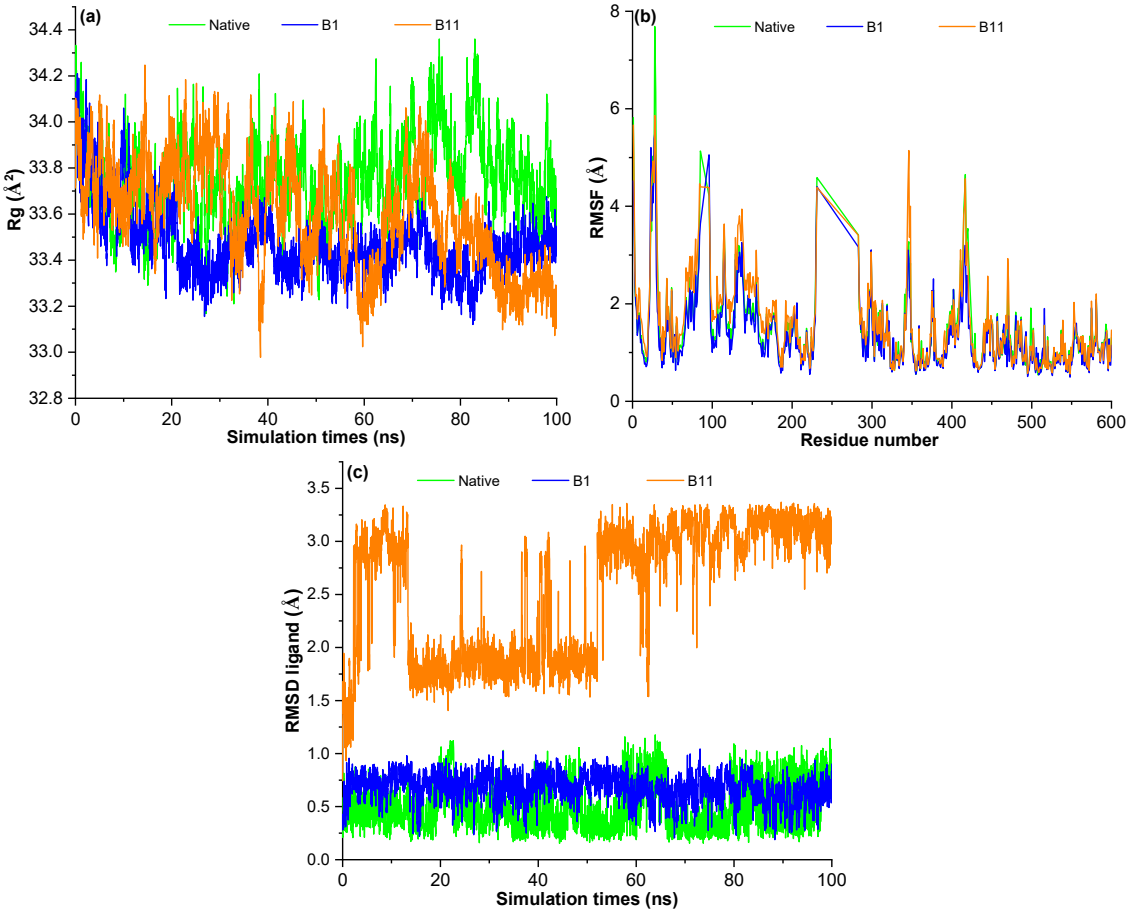

Fig 3. (a) Rg, (b) RMSF, and (c) RMSD of complex ligands **B1**, **B11**, and native against wt-*Pf*DHFR

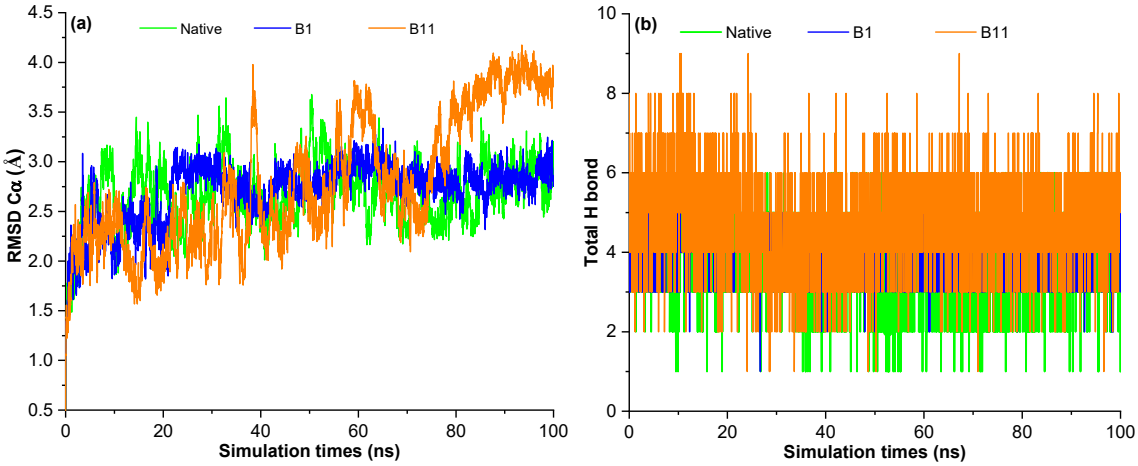

Fig 4. (a) RMSD C-alpha and (b) total H-bonds of complex ligand **B1**, **B11**, and native against wt-*Pf*DHFR

constant or stable RMSD after 20 ns, whereas wt-*Pf*DHFR-**B11** reached stability after 80 ns with higher RMSD values as shown in (Fig 4(a)).

This study also looked at the amount of hydrogen bonds during simulation to comprehend the complex's stability. Maintaining the high affinity between the ligand and protein depends on these hydrogen bonds [42]. During the simulation period, a total hydrogen bond analysis was performed on **B1** and **B11**. The total number of hydrogen bond interactions over 100 ns was

shown in (Fig 4(b)). For **B1**, four amino acid residues were consistently present since 0 ns, while for **B11**, five amino acid residues were consistently present. The hydrogen bonding interaction in the main region, also known as the typical hinge residue, and the extra residue were the two domains into which this interaction was separated. Although compound **B11** has more hydrogen bonds than compounds **B1** and native, the stability of the complex does not seem to depend solely on the number of hydrogen bonds.

■ CONCLUSION

ADME and toxicology prediction using for compounds derived from *S. rhombifolia* identified two compounds that meet Lipinski's, lead-likeness criteria, and inactive toxicology: 11-cryptolepine carboxylic acid (**B1**) and *N*-trans-feruloyltyramine (**B11**). The results of the molecular docking indicated that **B11** exhibits the highest potential as an inhibitor for the receptor protein wt-*Pf*DHFR, which plays a significant role in malaria disease, with a binding energy value of −8.41 kcal/mol. By using 100 ns molecular dynamics simulations, the stability of these compounds with *Pf*DHFR was further evaluated. These findings imply that **B1** and **B11** may be a viable option for more research and development for a malaria treatment. Based on these findings, we propose these substances as possible lead inhibitors of *Pf*DHFR for the management of malaria. To confirm these findings, more experimental research is required.

■ CONFLICT OF INTEREST

The authors declare that there is no conflict of interest

■ AUTHOR CONTRIBUTIONS

Herlina Rasyid designed the whole research and conducted molecular dynamics simulation. Arfansyah conducted the molecular docking analysis and molecular dynamics simulation, Anisa Sepyana plot and analyze the graphs. Muh Ade Artasasta conducted literature review and revised manuscript. Arfansyah, Anisa Sepyana, and Bahrun wrote and revised the manuscript. All authors agreed to the final version of this manuscript.

■ REFERENCES

[1] Zekar, L., and Sharman, T., 2025, *Plasmodium falciparum* Malaria, StatPearls Publishing, Treasure Island, FL, US.

[2] WHO, 2024, *World Malaria Report 2024: Addressing Inequity in the Global Malaria Response*, World Health Organization, Geneva.

[3] Handayani, L., and Fitriani, I., 2025, Review of *Plamodium vivax* malaria in Indonesia and Malaysia: Epidemiology of the infection and the presence of the vector across time, *Trop. J. Health Sci.*, 32 (2), 47–56.

[4] Alghamdi, J.M., Al-Qahtani, A.A., Alhamlan, F.S., and Al-Qahtani, A.A., 2024, Recent advances in the treatment of malaria, *Pharmaceutics*, 16 (11), 1416.

[5] Ahmad, I., Khan, H., Amin, M.U., Khalid, S., Behl, T., and Ur Rahman, N., 2021, An overview on the anticancer potential of punarnavine: Prediction of drug-like properties, *Oncologie*, 23 (3), 321–333.

[6] Bernardini, S., Tiezzi, A., Laghezza Masci, V., and Ovidi, E., 2018, Natural products for human health: An historical overview of the drug discovery approaches, *Nat. Prod. Res.*, 32 (16), 1926–1950.

[7] Ain, Q.T., Saleem, N., Munawar, N., Nawaz, R., Naseer, F., Ahmed, S., and Scotti, M., 2024, Quest for malaria management using natural remedies, *Front. Pharmacol.*, 15, 1359890.

[8] Ariefta, N.R., Sofian, F.F., Aboshi, T., Kuncoro, H., Dinata, D.I., Shiono, Y., and Nishikawa, Y., 2024, Evaluation of the antiplasmodial and anti-*Toxoplasma* activities of several Indonesian medicinal plant extracts, *J. Ethnopharmacol.*, 331, 118269.

[9] Liu, K.C.S.C., Yang, S.L., Roberts, M.F., Elford, B.C., and Phillipson, J.D., 1992, Antimalarial activity of *Artemisia annua* flavonoids from whole plants and cell cultures, *Plant Cell Rep.*, 11 (12), 637–640.

[10] Forkuo, A.D., Ansah, C., Mensah, K.B., Annan, K., Gyan, B., Theron, A., Mancama, D., and Wright, C.W., 2017, *In vitro* anti-malarial interaction and gametocytocidal activity of cryptolepine, *Malar. J.*, 16 (1), 496.

[11] Uzor, P.F., 2020, Alkaloids from plants with antimalarial activity: A review of recent studies, *Evidence-Based Complementary Altern. Med.*, 2020 (1), 8749083.

[12] Oliveira, M.S., Chaves, O.S., Cordeiro, L.V., Gomes, A.N.P., Fernandes, D.A., Teles, Y.C.F., da Silva, T.M.S., Freire, K.R.L., Lima, E.O., Agra, M.F., and de Souza, M.F.V., 2023, Indoquinoline alkaloids from *Sida rhombifolia* (L.) (Malvaceae) and antimicrobial evaluation of cryptolepinone derivatives, *J. Braz. Chem. Soc.*, 34 (2), 220–227.

[13] Aminah, N.S., Laili, E.R., Rafi, M., Rochman, A., Insanu, M., and Tun, K.N.W., 2021, Secondary metabolite compounds from Sida genus and their bioactivity, *Heliyon*, 7 (4), e06682.

[14] Kamdoum, B.C., Simo, I., Wouamba, S.C.N., Tchatat Tali, B.M., Ngameni, B., Fotso, G.W., Ambassa, P., Fabrice, F.B., Lenta, B.N., and Sewald, N., 2022, Chemical constituents of two Cameroonian medicinal plants: *Sida rhombifolia* L. and *Sida acuta* Burm. f. (Malvaceae) and their antiplasmodial activity, *Nat. Prod. Res.*, 36 (20), 5311–5318.

[15] Jiang, T., Chen, J., Fu, H., Wu, K., Yao, Y., Eyi, J.U.M., Matesa, R.A., Obono, M.M.O., Du, W., Tan, H., Lin, M., and Li, J., 2019, High prevalence of *Pfdhfr-Pfdhps* quadruple mutations associated with sulfadoxine-pyrimethamine resistance in *Plasmodium falciparum* isolates from Bioko Island, Equatorial Guinea, *Malar. J.*, 18 (1), 101.

[16] Morris, G.M., Huey, R., Lindstrom, W., Sanner, M.F., Belew, R.K., Goodsell, D.S., and Olson, A.J., 2009, AutoDock4 and AutoDockTools4: Automated docking with selective receptor flexibility, *J. Comput. Chem.*, 30 (16), 2785–2791.

[17] Hanwell, M.D., Curtis, D.E., Lonie, D.C., Vandermeersch, T., Zurek, E., and Hutchison, G.R., 2012, Avogadro: An advanced semantic chemical editor, visualization, and analysis platform, *J. Cheminf.*, 4 (1), 17.

[18] BIOVIA, Dassault Systèmes, 2020, *Discovery Studio Visualizer ver. 21.1.0.20298*, Dassault Systèmes, San Diego, US.

[19] Huang, C.C., Couch, G.S., Pettersen, E.F., and Ferrin, T., 1996, Chimera: An extensible molecular modeling application constructed using standard components, *Pac. Symp. Biocomput. 96*, 1 (724).

[20] Land, H., and Humble, M.S., 2018, YASARA: A tool to obtain structural guidance in biocatalytic investigations, *Methods Mol. Biol.*, 1685, 43–67.

[21] Daina, A., Michielin, O., and Zoete, V., 2017, SwissADME: A free web tool to evaluate pharmacokinetics, drug-likeness and medicinal chemistry friendliness of small molecules, *Sci. Rep.*, 7 (1), 42717.

[22] Banerjee, P., Kemmler, E., Dunkel, M., and Preissner, R., 2024, ProTox 3.0: A webserver for the prediction of toxicity of chemicals, *Nucleic Acids Res.*, 52 (W1), W513–W520.

[23] Rajendran, P., Rathinasabapathy, R., Chandra Kishore, S., and Bellucci, S., 2023, Computational-simulation-based behavioral analysis of chemical compounds, *J. Compos. Sci.*, 7 (5), 196.

[24] Pettersen, E.F., Goddard, T.D., Huang, C.C., Couch, G.S., Greenblatt, D.M., Meng, E.C., and Ferrin, T.E., 2004, UCSF Chimera—A visualization system for exploratory research and analysis, *J. Comput. Chem.*, 25 (13), 1605–1612.

[25] Wang, J., Wolf, R.M., Caldwell, J.W., Kollman, P.A., and Case, D. A., 2004, Development and testing of a general Amber force field, *J. Comput. Chem.*, 25 (9), 1157–1174.

[26] Dash, R., Ali, M.C., Dash, N., Azad, M.A.K., Hosen, S.M.Z., Hannan, M.A., and Moon, I.S., 2019, Structural and dynamic characterizations highlight the deleterious role of SULT1A1 R213H polymorphism in substrate binding, *Int. J. Mol. Sci.*, 20 (24), 6256.

[27] Mark, P., and Nilsson, L., 2001, Structure and dynamics of the TIP3P, SPC, and SPC/E water models at 298 K, *J. Phys. Chem. A*, 105 (43), 9954–9960.

[28] Gohlke, H., Hendlich, M., and Klebe, G., 2000, Knowledge-based scoring function to predict protein-ligand interactions, *J. Mol. Biol.*, 295 (2), 337–356.

[29] Laili, E.R., Aminah, N.S., Kristanti, A.N., Wardana, A.P., Rafi, M., Rohman, A., Insanu, M., and Tun, K.N.W., 2022, Comparative study of *Sida rhombifolia* from two different locations, *Rasayan J. Chem.*, 15 (1), 642–650.

[30] Karomah, A.H., Rafi, M., Septaningsih, A.A., Ilmiawati, A., Syafitri, U.D., Aminah, N.S., Insanu, M., and Rohman, A., 2023, UHPLC-Q-Orbitrap HRMS-based untargeted metabolomics of *Sida rhombifolia* leaves and stem extracts, *HAYATI J. Biosci.*, 30 (4), 770–778.

[31] Silvani, D., Wahyuni, W.T., Syafitri, U.D., Ilmiawati, A., Septaningsih, D.A., Insanu, M., Aminah, N.S., Rohman, A., and Rafi, M., 2023, LC-HRMS and FTIR-based metabolomics analysis and xanthine oxidase inhibitory evaluation of *Sida rhombifolia* with different drying methods, *Biocatal. Agric. Biotechnol.*, 52, 102833.

[32] Lipinski, C.A., Lombardo, F., Dominy, B.W., and Feeney, P.J., 2001, Experimental and computational approaches to estimate solubility and permeability in drug discovery and development settings, *Adv. Drug Delivery Rev.*, 46 (1), 3–26.

[33] Lipinski, C.A., 2004, Lead- and drug-like compounds: The rule-of-five revolution, *Drug Discovery Today: Technol.*, 1 (4), 337–341.

[34] Goodwin, J.T., Conradi, R.A., Ho, N.F.H., and Burton, P.S., 2001, Physicochemical determinants of passive membrane permeability: Role of solute hydrogen-bonding potential and volume, *J. Med. Chem.*, 44 (22), 3721–3729.

[35] Ahmad, S., Waheed, Y., Ismail, S., Bhatti, S., Abbasi, S.W., and Muhammad, K., 2021, Structure-based virtual screening identifies multiple stable binding sites at the RecA domains of SARS-CoV-2 helicase enzyme, *Molecules*, 26 (5), 1446.

[36] Petukh, M., Stefl, S., and Alexov, E., 2013, The role of protonation states in ligand-receptor recognition and binding, *Curr. Pharm. Des.*, 19 (23), 4182–4190.

[37] Gohlke, H., and Klebe, G., 2002, Approaches to the description and prediction of the binding affinity of small-molecule ligands to macromolecular receptors, *Angew. Chem., Int. Ed.*, 41 (15), 2644–2676.

[38] Fang, Y., 2012, Ligand–receptor interaction platforms and their applications for drug discovery, *Expert Opin. Drug Discovery*, 7 (10), 969–988.

[39] Di Stefano, E., Oliviero, T., and Udenigwe, C.C., 2018, Functional significance and structure–activity relationship of food-derived α-glucosidase inhibitors, *Curr. Opin. Food Sci.*, 20, 7–12.

[40] Glyakina, A.V., and Galzitskaya, O.V., 2020, How quickly do proteins fold and unfold, and what structural parameters correlate with these values ?, *Biomolecules*, 10 (2), 197.

[41] Bouricha, E.M., Hakmi, M., Akachar, J., Zouaidia, F., and Ibrahimi, A., 2022, *In-silico* identification of potential inhibitors targeting the DNA binding domain of estrogen receptor α for the treatment of hormone therapy-resistant breast cancer, *J. Biomol. Struct. Dyn.*, 40 (11), 5203–5210.

[42] Bulusu, G., and Desiraju, G.R., 2020, Strong and weak hydrogen bonds in protein–ligand recognition, *J. Indian Inst. Sci.*, 100 (1), 31–41.